Proceedings of ICFDP7:
Seventh International Conference of Fluid Dynamics and Propulsion
Dec. 18-20, 2001, Cairo, Egypt

ICFDP7-2001075

EXTERNAL VANES FLOATING PLUG NOZZLE THRUST VECTOR CONTROL

A.A. Hashem, Associate Professor
Aerospace Department, Cairo University
Cairo, Egypt

W. A. Aissa, Assistant Professor
Mechanical Power Department, High Institute of Energy
Aswan, Egypt

ABSTRACT

Interest is mounting for thrust vector control (TVC) as a mean for enhancing aircraft controllability and maneuverability. The design must cope with a range of operating conditions, and mission requirments. The use of external vanes post a convergent; and even classical convergent-divergent nozzles, may not be adequate for some applications. This inspired the evolution of a combined externally mounted vanes post a convergent nozzle with a central plug. The plug is floating i.e. free to rotate under the flow field of the deflected external vanes. This novel arrangement allows effective high nozzle pressure ratio applications, besides the ability to control both the thrust magnitude and direction. This is hopefully achieved without significant loss of vane senstivity as the exit nozzle area is varied considerably. The propsed arrangement was exprimentally tested at static conditions. The tests covered different nozzle pressure ratios, vane deflection angles, and plug locations relative to nozzle exit. The results indicated small increase in vanes side force and discharge cofficients. The main gain is expected to be due to the additional plug force. The vane sensitivity, due to the radial gap, was enhanced.

INTRODUCTION

TVC is emerging as a means of boosting aircraft maneuverability [1,5]. Nozzle exit vanes is an attractive method, especially for introducing TVC into existing engines. Several experimental investigations [2-7] have dealt with TVC using external vanes. It is thought that vectoring supersonic flow is less efficient in turning than lower velocity flow [5]. It is also obvious that employing exit vanes post a variable area, convergent divergent nozzle, with high nozzle pressure ratios, can suffer from operation in an overexpanded mode at low nozzle pressure ratios. In addition, applications requiring large divergent area variations, with fixed vanes hinge position; suffer from the increase in the radial gap for small areas. References [2,7] indicate that the vanes lose sensitivity as this gap increases.

This may lead to the conclusion that thrust vectoring is most effective for convergent nozzles having relatively low expansion ratios. However, the use of such nozzles becomes increasingly unsuitable at high nozzle pressure ratios.

Plug nozzles can deal effectively with high nozzle pressure ratio applications, since they better adapt to pressure ratios lower than design. A fixed direction axial plug may produce high flow resistance for the vane-deflected flow. In this arrangement, fig.1, a floating plug is installed. The plug is allowed to rotate freely in response to the aerodynamic forces created by the external vanes deflection.

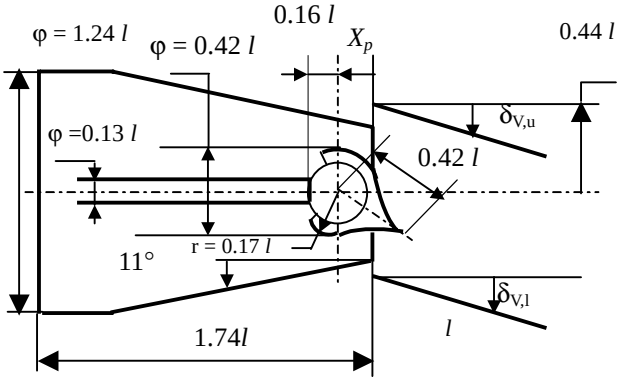

Fig.1 TVC floating plug nozzle.

Moreover, it is more effective to vary the nozzle throat by moving the plug axially, within properly chosen nozzle contour. Thus the vanes radial gap remains fixed, while simultaneously allowing for flow expansion around the plug, hence recovering a fraction of the lost thrust. Hopefully a reward may be gained on the side force, both on the vanes and on the central plug.

In the present study an experimental comparison is made between the performance of axisymmetric convergent nozzles under the effect of two externally mounted vanes, with and without a floating central plug. The plugless nozzle is shown in (fig.2).

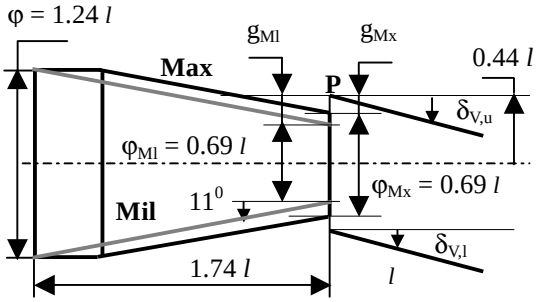

Fig. 2 TVC base line Convergent nozzle.

Nomenclature

A	Area
C_d	Nozzle discharge Coefficient
C_{Fa}	Axial force coefficient
C_{Fs}	Side force coefficient
C_{mh}	Hinge moment coefficient
Cp	Pressure coefficient
d	Diameter
F	Force
g	Radial gap
l	Vane length
M	Moment
$\dot{m}$	Mass flow rate
NPR	Nozzle pressure ratio
P	Pressure
q	Dynamic head
W	Vane width
δ_V	Vane deflection angle
γ	Ratio of specific heats
θ	Angular location

SUBSCRIPTS

a	Location a, actual, axial, atmospheric
b	Location b
c	Location c
h	Hinge
i	Ideal
0	Total
P	Plug
s	Side
ref	Reference
vp	Vane projected

TEST FACILITY

Tests are normally conducted in a steady state mode. However, there has been no available continuous air supply at the operating pressure range. Instead, air is supplied from a suitable tank, which is initially pressurized using clean dry air. Fig. 3 shows the layout of the test facility. Upon opening the tank outlet valve air passes through a standard venturi-meter to measure the mass flow rate. Then it flows into a plenum chamber where stagnation pressure and temperature P_o, T_o are measured. Upon passing through the nozzle, it is deflected by two externally mounted vanes. The vanes are deflected in and out the flow to control the engine thrust vector.

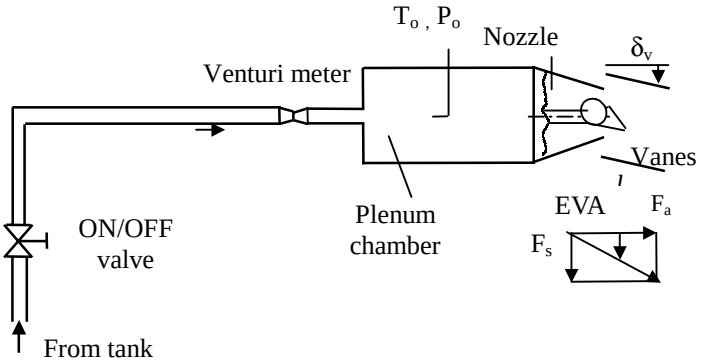

Fig. 3 Test rig layout.

The nozzle-plug dimensions are chosen such that the plug nozzle has a minimum throat area at plug location a, and maximum throat area at plug location c. Table 1 shows the three values considered for the plug axial position X_p, as shown by fig. 1.

Table 1 Plug axial locations.

Location	a	b	c
X_p/l	0	0.213	0.423

Spherical profile is employed around the plug center such that the nozzle throat area is not affected by plug deflections up to 30°. The vane length (*l*) is 50.8 mm. The vane pivots about point P such that it leaves a radial gap, which is required for the implementation of vane actuation system. The internal flow passage is a segment of a cone of a half cone angle; $\delta = 2.9^{\circ}$. The upper vane angle; $\delta_{v,u} = \delta_v + \delta$, while the lower vane angle; $\delta_{v,l} = \delta_v - \delta$. The upper vane is instrumented with sixteen pressure taps arranged in four rows of four holes each. Ref [7] gives details of the vane geometry.

The tests carried for the vanes post a baseline convergent nozzle [7] are used here as reference. Both military and maximum throat areas are considered, fig.2.

TRANSDUCERS AND DATA ACQUISITION SYSTEM

Twenty pressure transducers are utilized (one downstream the tank outlet valve, two for venturi meter static pressures, one for plenum chamber total pressure, and sixteen for vane inner surface pressure taps). The pressure transducers operating range is 0-10 bar gauge, with a non-linearity and hystress errors (percent of maximum) of ± 0.19 and 0.08, respectively.

A K type thermocouple is used for plenum chamber total temperature measurement, it has an error limit of 2.2°C or 0.75% (whichever is greater) above 0°C.

Fig. 4 shows a block diagram of the essential features of the data handling system. The system consists mainly of:
1) *Analog multiplexer*, which is a switch that can be digitally addressed to channel the analog data from each input to the amplifier and ADC 2) *Address decoder,* the DAS is connected

directly to the address and control buses of the computer. The address decoder is programmed by hardwired jumpers to respond to a particular set of addresses and control signals appearing on the buses 3) *Amplifier and ADC*, the unit has a built-in signal conditioning amplifier and ADC that operates on the data passed through the multiplexer. Thus any channel can be addressed through to the amplifier and ADC. The gain of the amplifier is externally adjusted. 4) *Tristate output latch*, since the output of the ADC is connected to the tristate latch, the DAS output lines are directly connected to the bus data of the computer. When a read operation takes place, the DAS enables the tristate buffers and load the data onto the data bus.

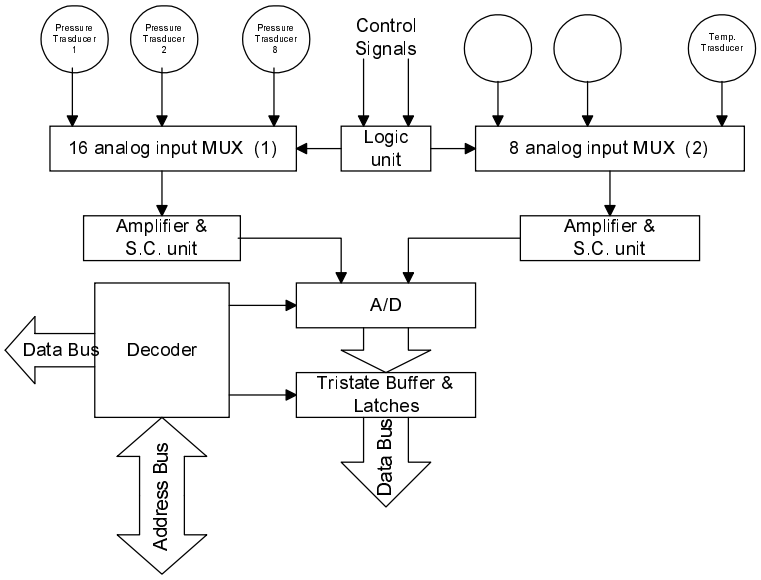

Fig.4 Data handling system.

ANALYSIS OF EXPERIMENTAL DATA

The measured sixteen pressure tap points are fitted using fifth order polynomial function to get vane internal surface pressure distribution. The pressure coefficient at axial distance x and circumferential distance s is defined by,

$$C_P(x,s) = (P - P_a)/P_a \quad (1)$$

The pressure coefficient distribution over the vane surface area is presented using three-dimensional plots for different nozzle pressure ratios and vane deflection angles.

The pressure at a point on the vane surface (x,s), as evaluated by the interpolation scheme is used to calculate the incremental forces and moments. Resultant force and hinge moment are evaluated for both the inside and outside vanes.

The resultant force is resolved into axial force (F_a) and side force (F_s).

Generalized form of aerodynamic coefficients (side force, axial force, and hinge moment coefficients) [7] are defined as:

$$F_s = q_{ref}\ A_{vp}\ C_{Fs} \quad , \quad F_a = q_{ref}\ A_{vp}\ C_{Fa} \quad (2)$$

$$M_h = q_{ref}\ A_{vp}\ l C_{mh} \quad (3)$$

where, q_{ref} is a reference dynamic head [7], given by

$$q_{ref} = P_0\,(1-(1/NPR)^{(\gamma-1)/\gamma})\ f(\gamma) \quad (4)$$

Where, $$f(\gamma) = \frac{\gamma}{(\gamma-1)}(2/(\gamma+1))^{1/(\gamma-1)} \quad (5)$$

These coefficients are function of some geometrical parameters. Besides the vane angle these include the following non-dimensional parameters: vane length to diameter ratio (l/d_{th}), vane aspect ratio (w/l) ,plug non-dimensional axial location (x_p/l), and radial gap ratio (g/d_{th}).

Effective vane angle representing the vane resultant force direction is defined as

$$EVA = \tan^{-1}(F_s/F_a) \quad (6)$$

The nozzle discharge coefficient is given by

$$C_d = \dot{m}_a / \dot{m}_i \quad (7)$$

RESULTS AND DISCUSSION

Fig. 5 presents samples of the inward moving vane pressure distribution; at NPR′s 6.0 and 3.0 for 30 degrees vane deflection angle, for maximum area convergent nozzle and floating plug nozzle (location c) configurations. The top end of the pressure coefficient axis corresponds to the largest pressure coefficient in the whole distribution. The figure indicates the pressure distributions of the floating plug nozzle resemble that of the corresponding plugless nozzle at the same throat area. The maximum pressure is slightly higher (5-17%) for the plug nozzle with the difference becoming more significant at high throat areas. There is also a slight gain for the maximum pressure at the low nozzle pressure ratio end.

Plug Nozzle Convergent nozzle

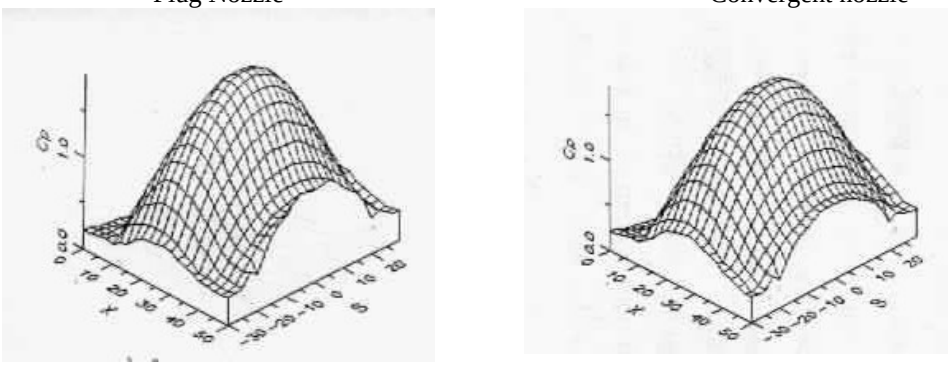

Min. area (location a), NPR=6

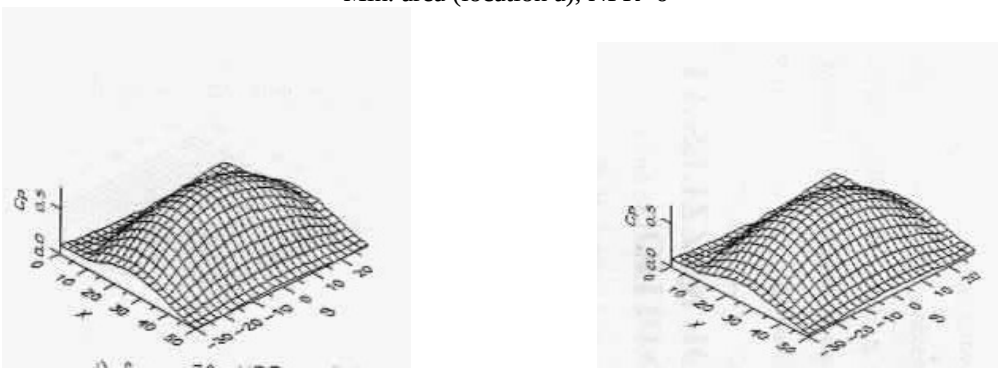

Min. area (location a), NPR=3

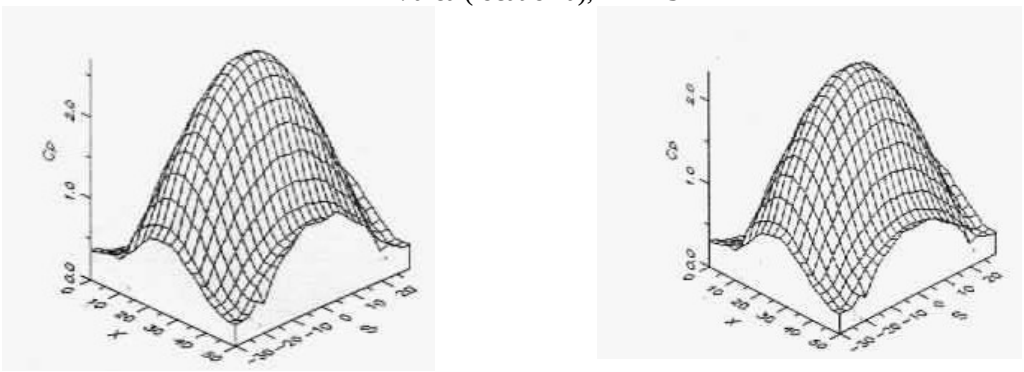

Max. area (location c), NPR=6

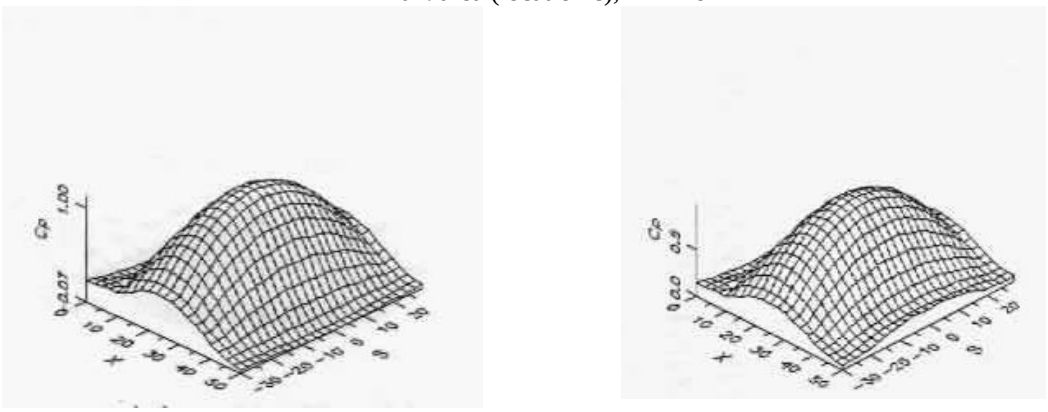

Max. area (location c), NPR=3

Fig. 5 Sample vane pressure distributions, vane deflection angle 30°.

Force and moment coefficients are used for comparing the aerodynamic performance of the floating plug nozzle with the base convergent nozzle. It is realized that the values of these coefficients have some scatter; due to variations of NPR, nevertheless a mean value may reasonably represent the actual

The side force coefficient of the floating plug and base nozzles is shown in fig. 6. It increases with the NPR and vane deflection angle. The plug nozzle develops significant gain in the side force over the base nozzle. This gain increases with the vane deflection angle. Operation at higher NPR′s produces slightly larger side force but has very small impact on the difference between the two nozzles.

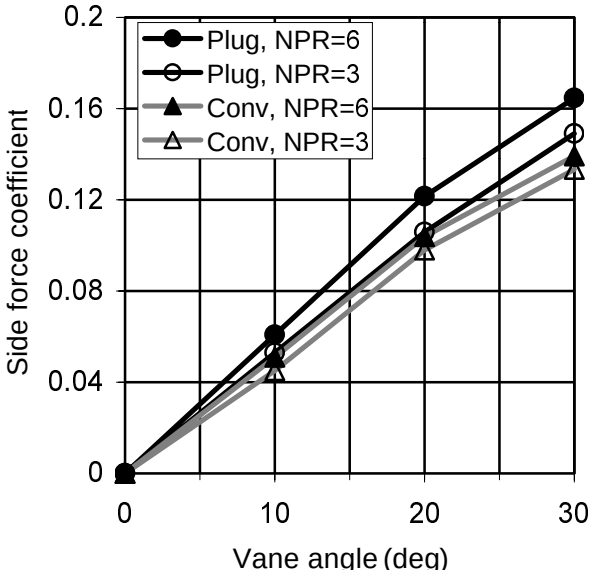

Fig. 6 Side force coefficient.

It is worth noting that, the plug introduces an additional force that contributes to the global side and axial force components. This force was not measured and was not included in the vane force components. The resultant plug force must pass through the plug hinge point, fig. 7. As the vanes deflect the floating plug rotates along with them such as to decrease the pressure on the side close to the inward moving vane and increase the pressure on the side close to the outward moving vane.

It is expected that the resultant force on the relevant part of the plug (the part downstream of the throat) is roughly passing along the line joining the plug trailing edge with the pivot point as shown in Fig. 7. This implies a definite axial force contribution; that adds to the thrust, and a likely favorable side force component (that adds to that of the vanes).

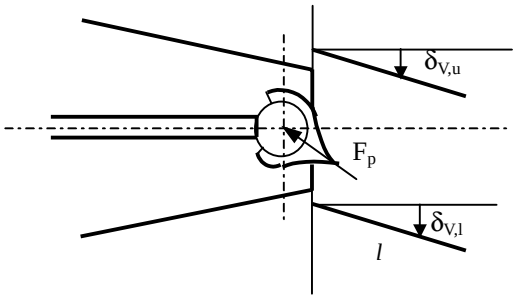

Fig. 7 Plug force.

With analogy to convergent nozzles, axial force for plug nozzles increases with NPR, and decreases by thrust vectoring, as the flow deflects away from the axial direction, Fig. 8. The Plug nozzle develops slightly larger axial force (drag) than the base nozzle. No significant effect for the NPR on the difference between the axial force of the nozzles is realized.

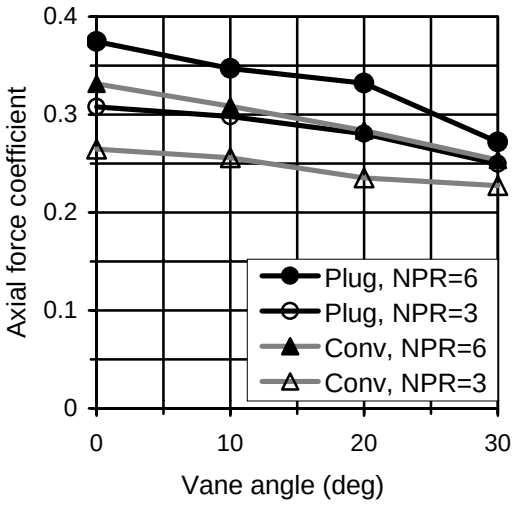

Fig. 8 Axial force coefficient, maximum throat area.

Fig. 9 indicates that the hinge moment of the floating plug nozzle with maximum throat area, location c, is higher than that of the maximum convergent nozzle. This is direct impact of the gain in side force. Since the variation of the hinge moment with the vane deflection angle remains almost linear for both types of nozzle, this implies similar movement of the center of pressure.

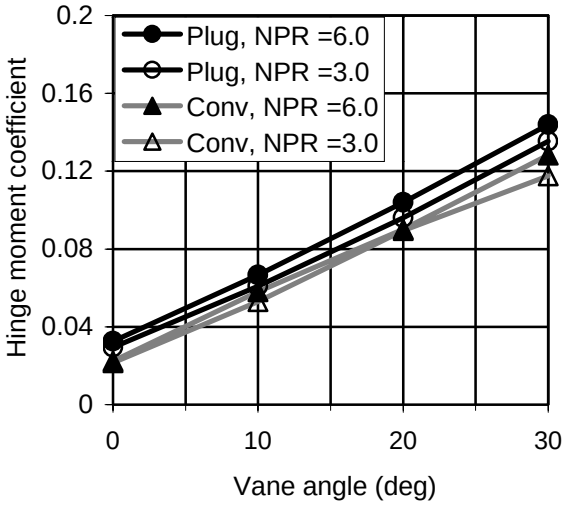

Fig. 9 Hinge moment coefficient, maximum throat area.

The effective vane angle is a useful measure of flow turning capability of the thrust vectoring arrangement. It gives an indication of the actual flow direction. The flow is expected to follow the geometric vane angle. Effective vane angles less than the geometric vane angles is indicative of loss in side force. While effective vane angles bigger than the geometric vane angles is indicative of loss in axial force.

Fig. 10 shows the variation of the effective vane angle for

Also indicated on the figure are two trend lines for the effective vane angle of the floating plug and base nozzles at minimum throat area. These lines indicate that, at minimum throat area, the effective vane angle of the floating plug nozzle is almost equal to the physical vane deflection angle, whereas

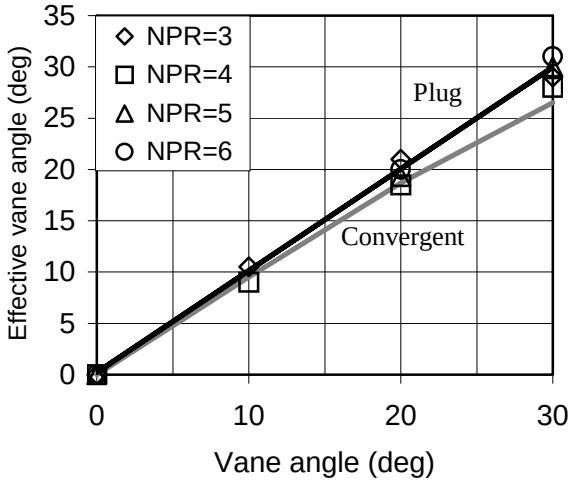

Fig. 10 Effective vane angle, min. throat area.

the convergent base nozzle shows a smaller effective vane angle, with the deviation from ideal increasing with the vane deflection angle. The nozzle pressure ratio has a small impact on the performance of both nozzles. This implies that the radial gap (which increases for the base convergent nozzle, at small throat areas) has its adverse effect on vane performance been reduced when the floating plug is introduced.

Fig.11 shows nozzle discharge coefficient for the floating plug and base nozzles. The discharge coefficient decreases slightly with the vane deflection angle and increases with the NPR. The figure also demonstrates significant gain for the plug nozzle all over the range.

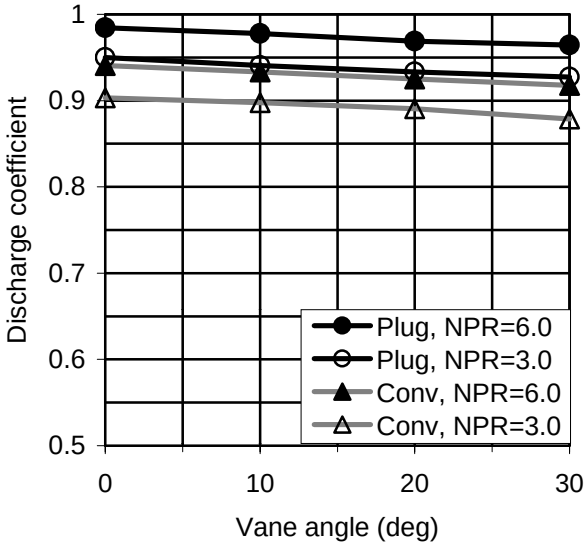

Fig. 11 Discharge coefficient, max. throat area.

CONCLUSIONS

A static test was conducted to evaluate thrust performance of axisymmetric convergent nozzles in which two externally vanes were mounted post the nozzle exit. A central floating plug was introduced. The floating plug self aligned itself to the flow as the external vanes were deflected. The plug was also used to vary the nozzle throat area via axial movement relative to nozzle exit. The tests covered different vane deflection angles, nozzle pressure ratio, and plug axial position. The results indicated that the NPR positively affected the values of the aerodynamic force and moment coefficients. A mean value for such coefficients demonstrated independence of the NPR

.

Proper self-deflection of the floating plug caused smooth turning of the flow, improving nozzle performance; represented by small increases of the vanes side force and nozzle discharge coefficients. At minimum throat areas, plug introduction reduced the adverse gap effect on the vane performance. However, the main gain of introducing the floating plug was thought to be due its favorable contribution

to the thrust at high nozzle pressure ratios, with a possible additional gain in side force.

REFERENCES

1. Gal-OR, B., "Fundamental Concepts of Vectored Propulsion," J. Propulsion, Vol. 6, No. 6, Nov-Dec, 1990.
2. Tamrat, B. F., and Antani, D. L., "Static Test Results of an Externally Mounted Thrust Vectoring Vane Concept", AIAA paper AIAA-88-3221, AIAA/ ASME/SAE/ASEE 24th Joint Propulsion Conference, Boston, Massachusetts, July 11-13, 1988.
3. Bare, E. A., and Reubush, D. E., "Static Internal Performance of a Two-Dimensional Convergent-Divergent Nozzle with Thrust Vectoring", NASA TP-2721, July 1987.
4. Berrier, B. L., and Mason, M. L., "Static Performance of an Axisymmetric Nozzle with Post-Exit Vanes for Multiaxis Thrust Vectoring," NASA TP-2800, May 1988.
5. Mason, M. L., and Berrier, B.L., "Static Performance of Non axisymmetric Nozzles with Yaw Thrust-Vectoring," NASA TP-2813, May 1988.
6. Aissa, W. A., "Thrust Control Using Combined Vanes and Plug Arrangements," Ph. D Thesis, Cairo University, May 1999.
7. Aissa, W. A., and Hashem, A. A.. "Experimental Analysis of Thrust Control Using External Vanes", Fifteenth International Symposium on Airbreathing Engines, ISABE 2001-1186, Sep. 2001.